Vibrational mode-specific dynamics of the $F(^2P_{3/2}) + C_2H_6 \rightarrow HF + C_2H_5$ reaction

Dóra Papp and Gábor Czakó

Vibrational mode-specific dynamics of the F(^{2}P$_{3/2}$) + C$_2$H$_6$ → HF + C$_2$H$_5$ reaction

Dóra Papp[a] (ID) and Gábor Czakó[a] (ID)
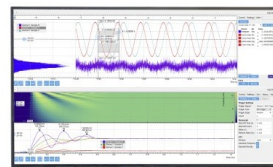
AFFILIATIONS

MTA-SZTE Lendület Computational Reaction Dynamics Research Group, Interdisciplinary Excellence Centre and Department of Physical Chemistry and Materials Science, Institute of Chemistry, University of Szeged, Rerrich Béla tér 1, Szeged H-6720, Hungary

[a]Authors to whom correspondence should be addressed: dorapapp@chem.u-szeged.hu and gczako@chem.u-szeged.hu

ABSTRACT

We investigate the competing effect of vibrational and translational excitation and the validity of the Polanyi rules in the early- and negative-barrier F(^{2}P$_{3/2}$) + C$_2$H$_6$ → HF + C$_2$H$_5$ reaction by performing quasi-classical dynamics simulations on a recently developed full-dimensional multi-reference analytical potential energy surface. The effect of five normal-mode excitations of ethane on the reactivity, the mechanism, and the post-reaction energy flow is followed through a wide range of collision energies. Promoting effects of vibrational excitations and interaction time, related to the slightly submerged barrier, are found to be suppressed by the early-barrier-induced translational enhancement, in contrast to the slightly late-barrier Cl + C$_2$H$_6$ reaction. The excess vibrational energy mostly converts into ethyl internal excitation while collision energy is transformed into product separation. The substantial reaction energy excites the HF vibration, which tends to show mode-specificity and translational energy dependence as well. With increasing collision energy, direct stripping becomes dominant over the direct rebound and indirect mechanisms, being basically independent of reactant excitation.

Published under an exclusive license by AIP Publishing. https://doi.org/10.1063/5.0069658

INTRODUCTION

The mode- and bond-selective control of a reaction has always been in the focus of chemistry. The first rules of reaction dynamics related to the relative efficiency of vibrational and translational excitation of a simple A + BC → AB + C three-atom reaction were established by Polanyi in 1987,[1] and say that this efficiency is determined by the position of the transition state (TS) along the reaction coordinate. That is, translational energy promotes a chemical reaction that needs to overcome a reactant-like "early" barrier, while vibrational excitation of the reactant BC molecule enhances the reactivity of a "late-barrier" reaction having a product-like TS with an elongated B–C bond.[1] Schatz and co-workers started to investigate more complicated systems, namely, the H + HOD → H$_2$ + OD reaction, for which, based on quasi-classical trajectory (QCT) simulations, they predicted that exciting the OH stretching mode with five quanta enhances more effectively the reactivity than the OD stretching excitation.[2] These predictions were also confirmed by experiments of the groups of Crim[3,4] and Zare.[5] A decade later, the full-dimensional quantum mechanical description of this reaction became possible as

well, and the quantum dynamics results of Zhang and Light showed good agreement with experiments.[6]

As the size of the studied reactive chemical systems[7–10] increased, several departures from the Polanyi rules were revealed, mainly due to the quick growth in the number of the internal degrees of freedom. Experiments of Liu and co-workers investigating the atom + methane reaction family showed that exciting the CH-stretching mode in the late-barrier Cl + CHD$_3$ reaction has a smaller effect on promoting the reaction than translational excitation,[11] and the CH-excitation prevents the cleavage of the C–H bond in the F + CHD$_3$ reaction.[12] Important developments in the fitting methods of potential energy surfaces (PESs)[13,14] allowed to explain these unexpected experimental findings by performing QCT simulations. Accordingly, Czakó and Bowman revealed that in the case of the Cl + CHD$_3$ reaction at low collision energies, the Polanyi rules are counteracted by the guiding effect of the entrance-channel van der Waals minima.[15] Several mode-specific QCT studies on accurate *ab initio* analytical potential energy surfaces (PESs) were then performed for this class of reactions, including the F + CHD$_3$,[16,17] O + CH$_4$,[18] and Br + CH$_4$[19] systems. Mode-specificity in atom

+ methane reactions was also studied by quantum dynamics calculations.[20–27] Successful attempts toward the generalization of the Polanyi rules were also made by introducing the Sudden Vector Projection model by Jiang and Guo.[28,29]

Following some early experimental and theoretical studies,[30–39] by the 2010s, theoretical reaction dynamics became capable of accurately modeling even more complex systems, containing more than six atoms.[40,41] Such investigations involved the O + C_2H_4,[42] OH + CH_4,[43] and OH + CH_3OH[44] reactions and arrived at the detailed dynamical studies of the nine-atomic F/Cl + C_2H_6 → HF/HCl + C_2H_5 reactions carried out by the present authors and providing very good agreement with experiments.[45,46] Mode-specificity in the dynamics of the seven-atomic F + CH_3OH,[47] and very recently in the Cl + C_2H_6 → HCl + C_2H_5 reaction,[48] featuring a submerged slightly late-barrier, was also investigated. Note that the kinetics and dynamics of the F/Cl/O + C_2H_6 reactions were previously investigated on force-field-based PESs as well.[49–52]

Here, we investigate the competition between vibrational and translational excitation in the $F(^2P_{3/2})$ + C_2H_6 → HF + C_2H_5 nine-atomic reaction featuring an early barrier slightly submerged below the reactants. Five selected vibrational modes of ethane are excited, one at a time and each with one quantum, during the QCT simulations carried out at four different collision energies and by using the spin–orbit corrected MRCI-F12 PES recently developed for the title reaction by the present authors.[46] The effects of the different kinds of excitations on the reactivity, the reaction mechanism, and the post-reaction distribution of energy are monitored, and the validity of the Polanyi rules is inspected as well. In addition, a comparison with the mode-specific dynamics of the negative but slightly late-barrier Cl + C_2H_6 H-abstraction reaction is also provided.

COMPUTATIONAL DETAILS

Quasi-classical dynamics simulations for the $F(^2P_{3/2})$ + C_2H_6 → HF + C_2H_5 reaction are performed at 1.0, 3.2, 10.0, and 20.0 kcal/mol collision energies on a MRCI-F12 PES[46] developed by the present authors using the Robosurfer program package[53] recently designed for automatically generating and improving permutationally invariant[13,54] reactive PESs. We investigate the effect of five different reactant normal mode excitations, each with one quantum [the v_3 C–C stretching (2.83), the v_6 CH_3-deformation (3.93), the v_1 symmetric CH-stretching (8.75), the v_5 asymmetric CH-stretching (8.77), and the v_7 degenerate CH-stretching (9.02) modes with fundamental harmonic energies given in kcal/mol in parentheses], and

compare the results with those obtained for the unexcited reaction. The motions corresponding to these normal-mode vibrations are represented in Fig. 1. The initial vibrational energy is set by using the standard normal-mode sampling.[55]

The initial distance of the F atom and the center of mass of the ethane molecule is $\sqrt{x^2 + b^2}$, where $x = 16$ bohr and the b impact parameter, the distance between the velocity vectors of the reactants, is varied between 0 and b_{max}, where the reaction probability vanishes, with a step size of 1 bohr. The orientation of the reactants is sampled randomly. The time step used for propagating the trajectories is 0.0726 fs, and a trajectory ends when the longest atom–atom distance becomes larger than the longest initial one by 1 bohr. We run 500 trajectories for each impact parameter-collision energy-mode excitation combination.

Integral cross sections (ICSs) are calculated by using a b-weighted numerical integration of the opacity functions (the reaction probabilities as a function of b) in the case of each reactant mode excitation and also for the unexcited reaction at each collision energy. We use different zero-point-energy (ZPE) constraints for the ICSs: (1) Soft—the sum of the classical vibrational energy of the ethyl radical and the internal energy of the HF product must be higher than the sum of the harmonic ZPE of the ethyl radical and the anharmonic ZPE of HF corresponding to its actual rotational state. (2) Hard—the above restrictions are set separately for each product. (3) "Ethyl"—the restriction is only set for the ethyl radical. Variationally calculated rovibrational energy levels of HF are taken from Ref. 14. The product scattering angle distributions are determined by binning the cosine of the angle (θ) between the relative velocity vectors of the center of masses of the reactants and the products into five equidistant bins, where $\cos(\theta) = -1$ corresponds to backward scattering. The rotational quantum number of HF is determined as described in Ref. 45, and the vibrational quantum number of HF is that of the anharmonic rovibrational energy level corresponding to the actual rotational state of HF nearest to its classical internal energy.

RESULTS AND DISCUSSION

We investigate the vibrational mode-specificity in the $F(^2P_{3/2})$ + C_2H_6 → HF + C_2H_5 reaction by carrying out QCT simulations at 1.0, 3.2, 10.0, and 20.0 kcal/mol collision energies using an analytical MRCI-F12 PES[46] by exciting five different normal modes of ethane. The schematic potential energy landscape of the reaction is shown in Fig. 2 comparing benchmark all-electron CCSDT(Q)/complete-basis-set-quality[56] and MRCI-F12/aug-cc-pVDZ classical energies[46]
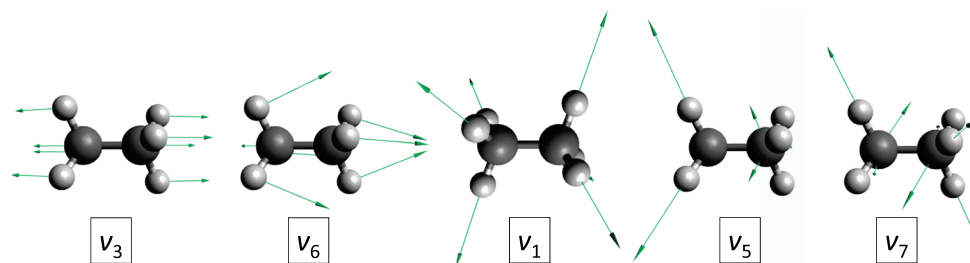

FIG. 1. Schematic representation of the normal-mode vibrations of ethane studied in the present work: v_3 C–C stretching, v_6 CH_3-deformation, v_1 symmetric CH-stretching, v_5 asymmetric CH-stretching, and v_7 degenerate CH-stretching, where v_x [x = 1, 3, 5, 6, 7] refer to the standard Mulliken notations.
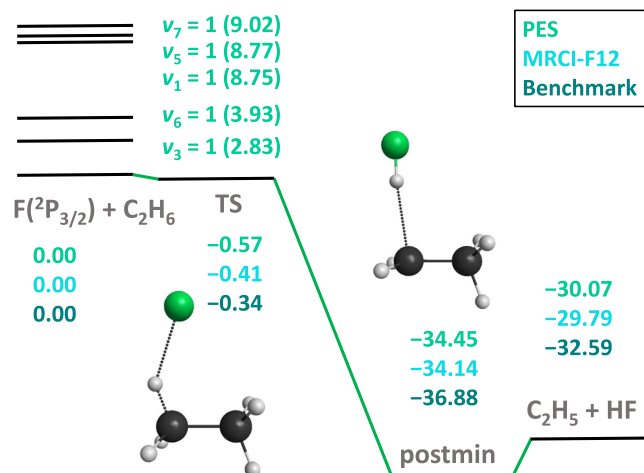
FIG. 2. Schematic potential energy surface of the F($^2P_{3/2}$) + C$_2$H$_6$ → HF + C$_2$H$_5$ reaction comparing benchmark[56] and MRCI-F12/aug-cc-pVDZ classical relative energies[46] (kcal/mol) of the stationary points with those obtained on our recently developed PES[46] and showing five single-excited vibrational energy levels (kcal/mol; in parentheses) of ethane obtained on the PES. Adapted with permission from D. Papp and G. Czakó, J. Chem. Phys. **153**, 064305 (2020). Copyright 2020 AIP Publishing LLC.

relative to the spin–orbit ground state of the reactants with those obtained on the PES. We can see that in the exit channel the MRCI-F12 method somewhat struggles to reproduce the benchmark energies, although it gives a correct description of the energy gap between the post-reaction minimum and the products. The good agreement between the MRCI-F12 and PES energies, on the other hand, highlights the accuracy of the fitting. The reaction is highly exothermic with a reaction energy of −32.6 kcal/mol and features a slightly submerged (−0.3 kcal/mol classical and −1.0 adiabatic[56]) barrier with a strongly reactant-like TS structure (the H–F distance is 1.94 Å)[56] and a deep (−36.9 kcal/mol) product-like minimum in the exit channel. The single-excited harmonic vibrational energy levels of ethane are also shown in Fig. 2.
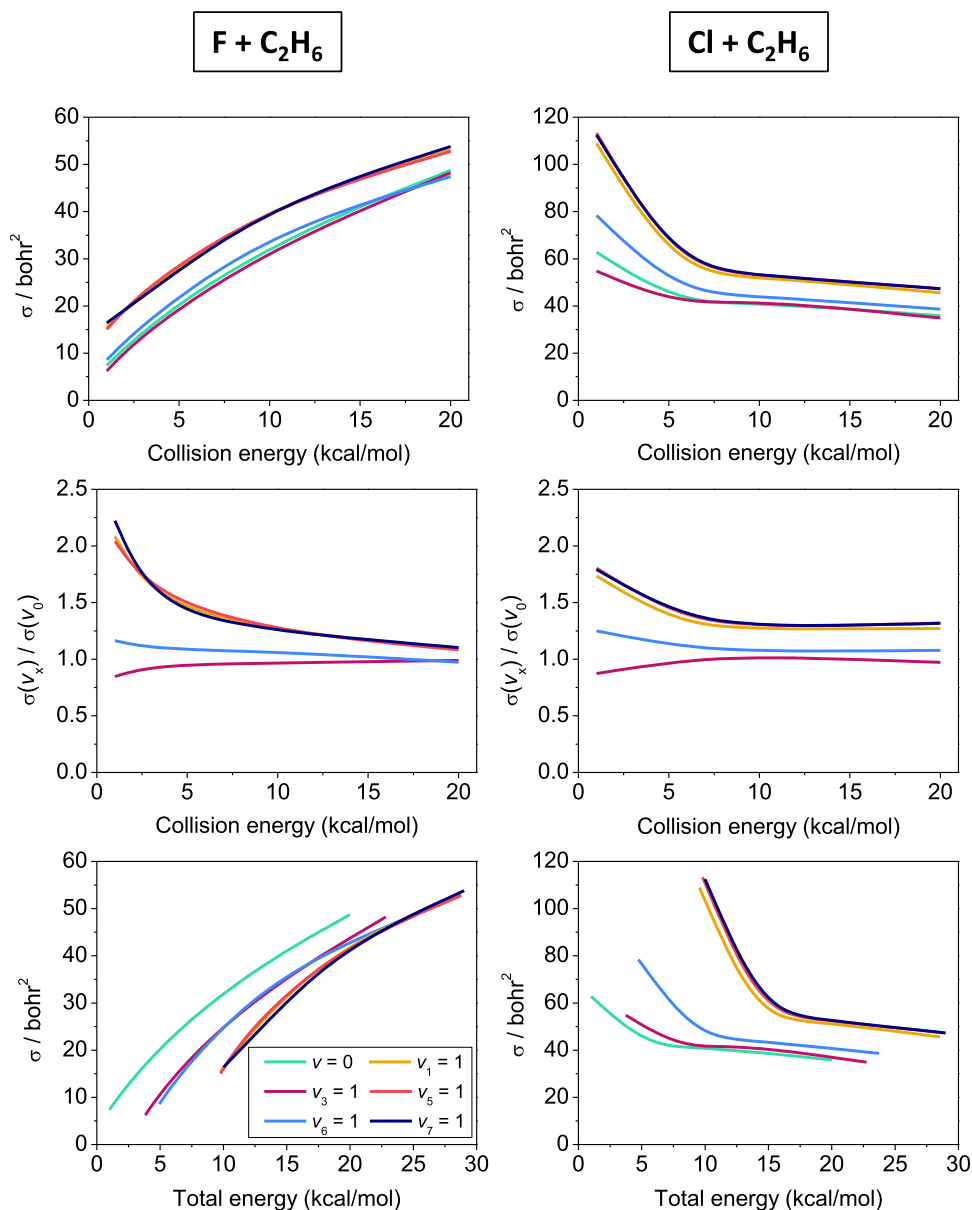
Integral cross sections as a function of collision energy, i.e., the excitation functions, obtained with different ZPE-restrictions are plotted in Fig. 3 and feature the same monotonically increasing shape for all ethane normal mode excitations and for the unexcited reaction as well. This shape, on one hand, is the result of the competition between the effects of the reactant-like structure and the submerged nature of the reaction barrier: The former predicts, based on the Polanyi rules, a strong enhancement in reactivity with increasing translational excitation, whereas the latter would suggest increasing reactivity with longer interaction time, available at lower collision energies. From Fig. 3, it is clear that the early barrier
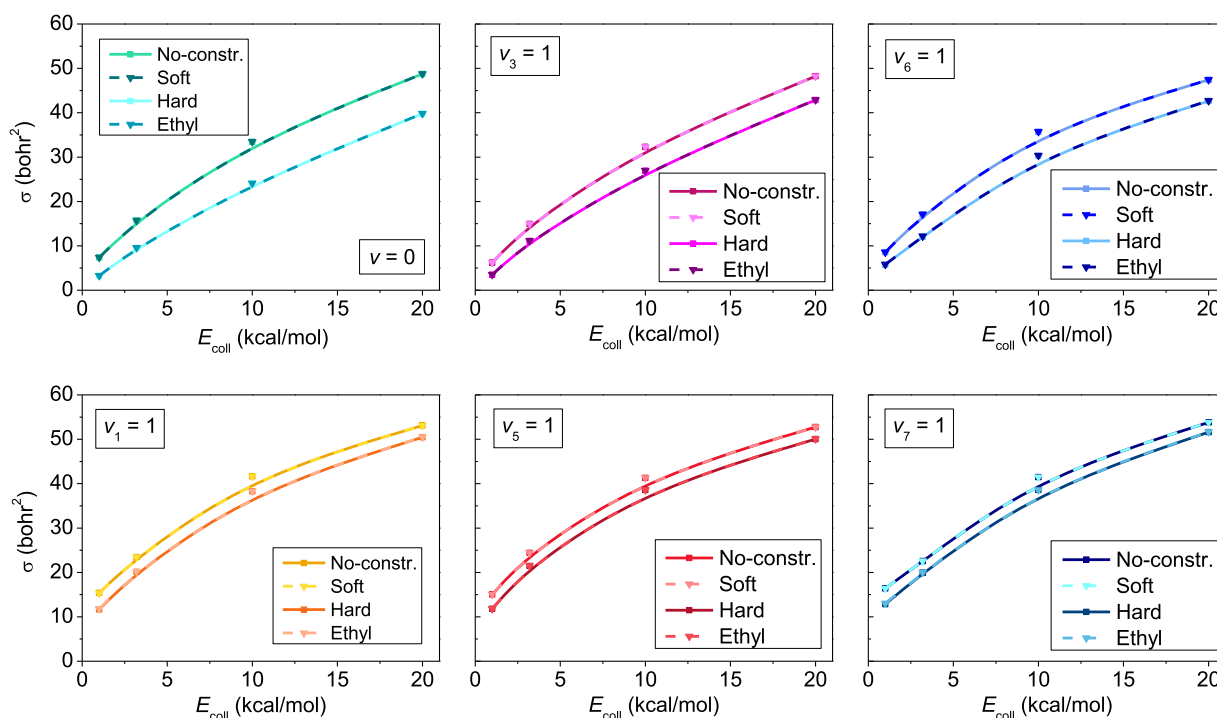
FIG. 3. Integral cross sections for the F + C$_2$H$_6$($v = 0$, $v_x = 1$) → HF + C$_2$H$_5$ [$x = 1, 3, 5, 6, 7$] reactions as a function of collision energy obtained with different ZPE constraints (for more details, see the text).

controls the reaction. On the other hand, a centrifugal barrier also emerges at nonzero b values, which might turn the slightly negative barrier (-0.6 kcal/mol on the PES) into a small positive value, resulting in increasing reactivity with increasing collision energy. Due to the intramolecular vibrational redistribution (IVR), one can expect some loss in the initial vibrational excitation; however, it has been shown for the $Cl + C_2H_6 \rightarrow HCl + C_2H_5$ reaction that IVR does not prevent the system from keeping its mode-specific character.[48] In Fig. 3, it can be seen that the soft ZPE constraint gives essentially

the same ICS values as if we do not apply any ZPE-restriction for the products. The reactant-like TS geometry accounts for this phenomenon as well, by making the HF molecules to form in highly excited vibrational states due to the elongated H–F distance at the TS, which compensates the internal energy of the ZPE-violating ethyl radical products in the case of the soft constraint. This finding is also responsible for the practically identical results provided by the hard and the "ethyl" ZPE-restrictions because in the case of the hard constraint, we only discard trajectories due to

FIG. 4. Integral cross sections for the $F/Cl + C_2H_6(v = 0, v_x = 1) \rightarrow HF/HCl + C_2H_5$ [$x = 1, 3, 5, 6, 7$] reactions as a function of collision energy (upper panel) and total energy (lower panel), as well as enhancement factors corresponding to each reactant excitation with respect to the ground-state reaction as a function of collision energy (middle panel). The results for the $Cl + C_2H_6$ reaction are taken from Ref. 48.

ZPE-violation in the ethyl radical. In Fig. 3, we can observe that when the CH-stretching modes are excited in ethane, the hard-restricted excitation functions approach the ones obtained without ZPE-restriction, which indicates that the excess energy pumped into the CH vibrations at least partly flows into the ethyl radical; this way, the number of the discarded trajectories and, thus, the difference between the constrained and non-constrained excitation functions significantly decrease. This energy flow is less pronounced in the case of v_3 and v_6 excitations. At 1.0 kcal/mol collision energy, where enough time is available for the CH-stretching vibrational excitation to take effect, it gives rise to about a double increase in the non-constrained reactivity relative to the

unexcited reaction, while toward higher collision energies, this increment decreases significantly.

In the upper panels of Fig. 4, the ICSs (without ZPE constraint) as a function of collision energy of the F/Cl + C_2H_6 → HF/HCl + C_2H_5 reactions are shown. The obvious difference in the shapes of the excitation functions of the above two reactions is partly due to the vastly different potential energy landscapes, especially the positions of the TSs. That is, the early-barrier F + C_2H_6 reaction is essentially promoted by translational excitation, while the reactivity of the slightly late-barrier Cl + C_2H_6 reaction can be clearly enhanced by vibrational excitation, in accordance with the predictions of the Polanyi rules. However, the above-mentioned
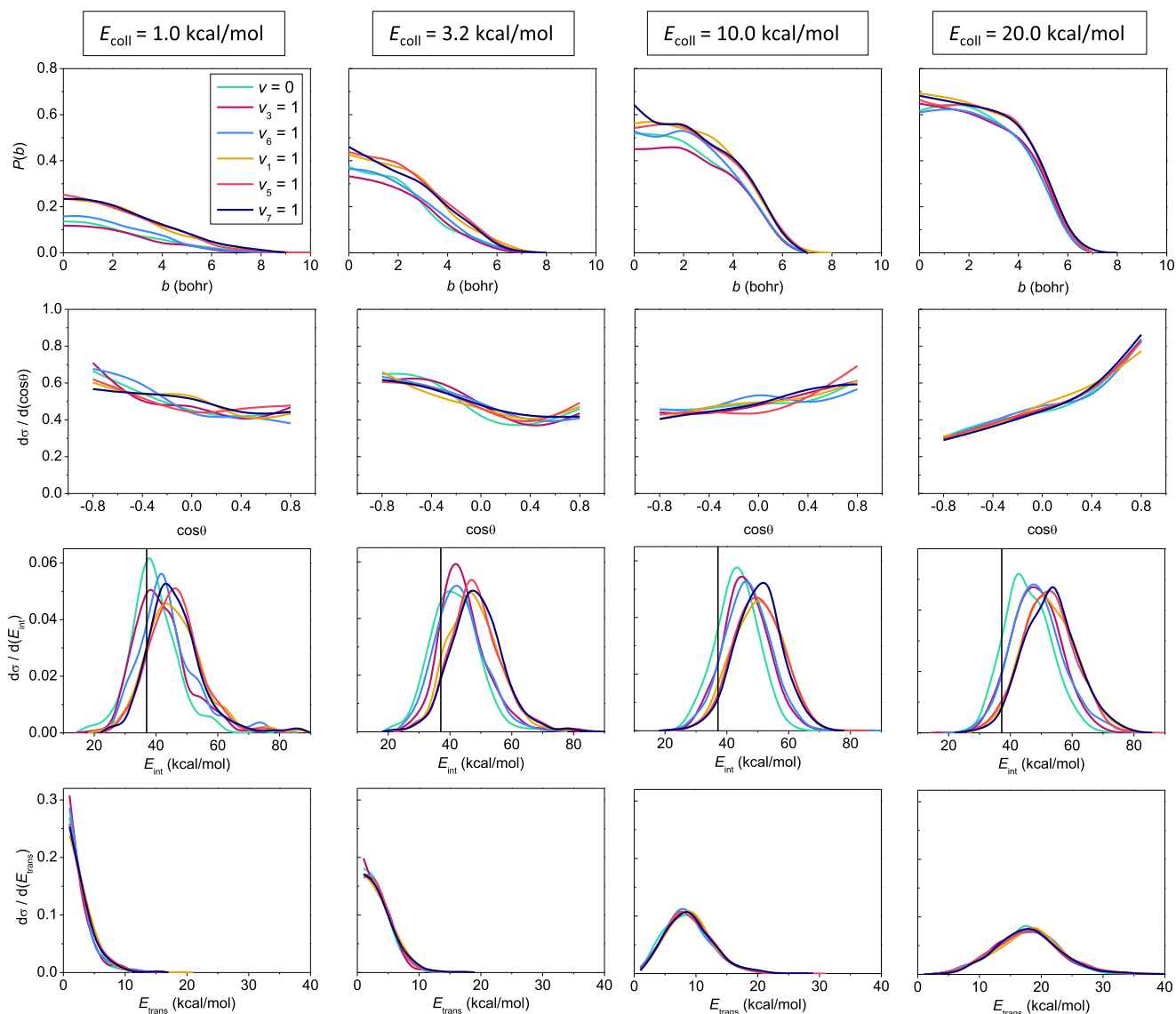
FIG. 5. Opacity functions (topmost panel), normalized product scattering angle distributions (upper middle panel), normalized internal energy distributions of the ethyl radical (lower middle panel, where the vertical line refers to the ZPE of the ethyl radical, 37.8 kcal/mol), and normalized relative translational energy distributions of the products (lowest panel) of the F + $C_2H_6(v = 0, v_x = 1)$ → HF + C_2H_5 [x = 1, 3, 5, 6, 7] reactions at 1.0, 3.2, 10.0, and 20.0 kcal/mol collision energies.

centrifugal barrier can also impact the reactivity, contributing to the monotonically increasing shape of the excitation functions of the $F + C_2H_6$ reaction. On the other hand, the much deeper barrier (-2.6 kcal/mol) of the $Cl + C_2H_6$ reaction, where the centrifugal barrier might have only a minor effect, results in a decaying shape of its excitation functions, which underlines the importance of the promoting effect of reaction time in the case of a submerged barrier, where, if the collision energy is low enough, and therefore the system spends enough time near the TS-region, the reaction will be more likely to occur.[45,48] However, if we inspect the middle panels of Fig. 4, it suggests that a similar enhancement can be observed due to vibrational excitation for the two reactions. This is, of course, an incomplete point of view since the translational or vibrational contribution to the total energy can be critical regarding reaction promotion. Therefore, we also plot the ICS values as a function of the total initial energy, which gives us more insight. If we consider a total energy of 10.0 kcal/mol for the $F + C_2H_6$ reaction in the case of v_3 and v_6 mode excitations, where about 30%–40% of the available energy is in the vibrational degrees of freedom, we can see a 20% drop in the ICS with respect to the unexcited reaction. Moreover, when the CH-stretching modes are excited in ethane, where 90% of the 10 kcal/mol total initial energy is stored in vibration, the ICS experiences a 50% decrease. This trend becomes less pronounced as the collision energy increases, e.g., at 20.0 kcal/mol total energy, the ICSs of the excited reactions do not differ significantly, and the unexcited ethane reacts only slightly more efficiently than the excited molecule. Thus, it is apparent that translational energy promotes much more effectively the early-barrier $F + C_2H_6$ H-abstraction reaction than vibrational energy. In contrast, in the case of the rather late-barrier $Cl + C_2H_6$ reaction, the excitation of the low-frequency v_6 mode already improves the reactivity by around 15%, while the CH-excitations cause an almost triple increase in reactivity at a total energy of 10 kcal/mol. The vibrational promotion of the $Cl + C_2H_6$ reaction due to CH-excitation decreases considerably with increasing collision energy, resulting in a ~40% increment at 20.0 kcal/mol, while the enhancement induced by the v_6 mode excitation almost vanishes, probably due to the shorter interaction time caused by faster collisions. Evidently, in this case, vibrational excitation wins over the effect of increasing translational energy, which, in fact, acts against the overall reactivity due to the more negative barrier with respect to that of the $F + C_2H_6$ reaction. As seen in the middle panels of Fig. 4, lower initial translational energies, and therefore longer collision time, even despite IVR, help vibrational excitation to increase reactivity in both reactions. Interestingly, the inhibiting effect of the v_3 CC-stretching mode excitation can be observed also in both cases at low collision energies.

As inspecting the opacity functions shown in the upper row of Fig. 5, we can observe a significant enhancement mainly at smaller impact parameters for the title reaction with increasing collision energy, while the b_{max} values do not change considerably, and only a minor mode-specificity is seen, predominantly at lower energies. The scattering angle distributions of the products, plotted in the second row of Fig. 5, which show a slight backward preference at low energies and a clear forward-scattering pattern at higher energies, along with the increasing reaction probabilities at larger b values with increasing collision energy, indicate an excessively dominant stripping mechanism over the direct rebound and indirect scenarios, which are mainly observed at low collision energies. The internal

energy distributions of the ethyl radical product, plotted in the third row of Fig. 5, feature clear mode-specificity with maxima shifting toward higher energies with nearly the value of the excess vibrational energy while showing only a slight collision energy dependence. This
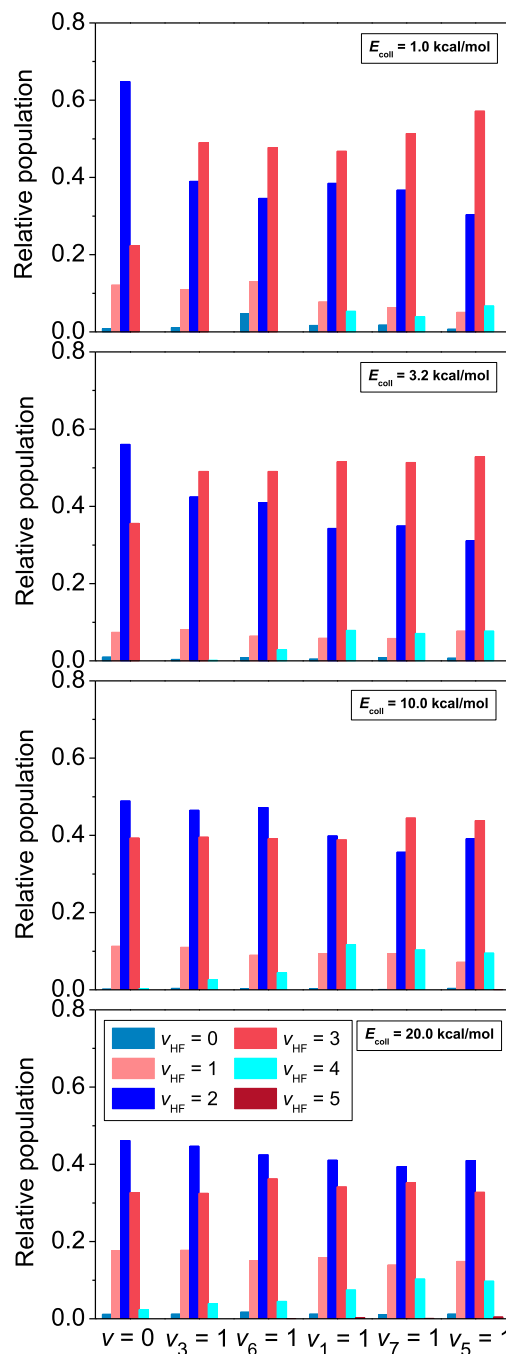
FIG. 6. Vibrational state distributions of the HF product of the $F + C_2H_6(v = 0, v_x = 1) \rightarrow HF + C_2H_5$ [$x = 1, 3, 5, 6, 7$] reactions at 1.0, 3.2, 10.0, and 20.0 kcal/mol collision energies obtained with hard ZPE-restriction.
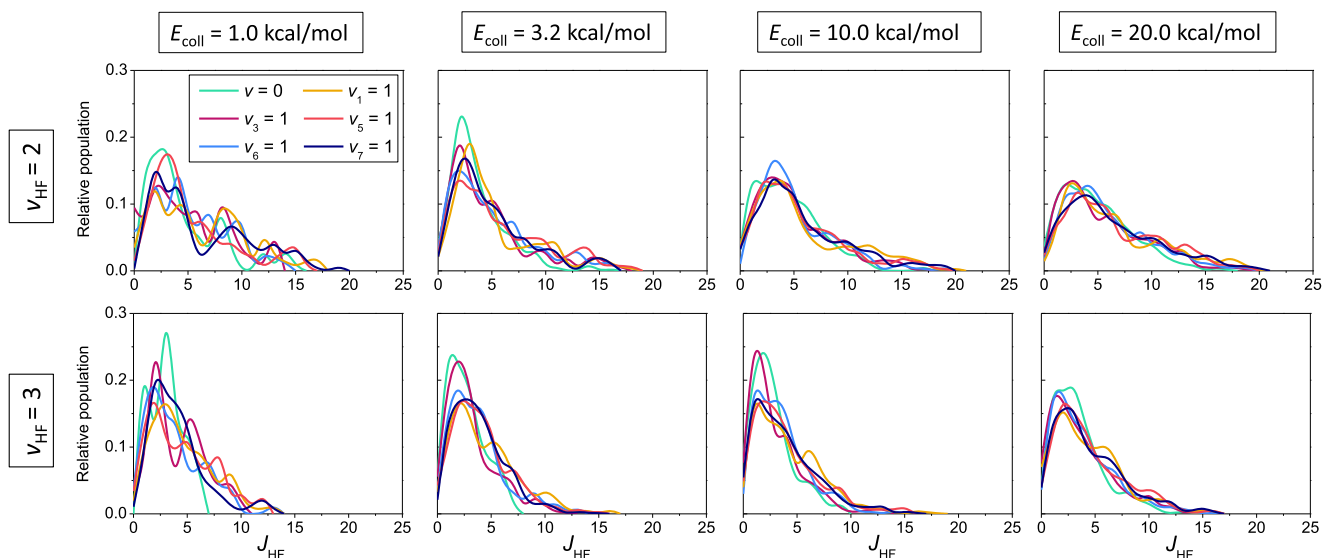
FIG. 7. Rotational state distributions of the HF($v_{HF} = 2$) and HF($v_{HF} = 3$) products of the F + C_2H_6($v = 0$, $v_x = 1$) → HF + C_2H_5 [x = 1, 3, 5, 6, 7] reactions at 1.0, 3.2, 10.0, and 20.0 kcal/mol collision energies obtained with hard ZPE-restriction.

shift becomes more and more apparent as collision energy increases. In contrast, the maxima of the relative translational energy distributions (fourth row of Fig. 5) are clearly blue-shifted, approximately with the values of the collision energy increments, and the distributions are also widened with increasing collision energy, regardless of the ethane mode excitations. Thus, while most of the vibrational excitation energy remains in the ethyl radical, the initial translational energy mostly converts into product recoil. From the ethyl internal energy distributions, it is clear that a significant number of trajectories are ZPE violating, especially at low collision energies, which underlies the application of the different ZPE constraints for the ICS values.

In Fig. 6, we show the vibrational state distributions of the HF product obtained with hard ZPE-restriction for all the initial ethane normal mode excitations. We have seen that the excess vibrational energy given to ethane mainly remains in the ethyl radical, and the collision energy tends to flow into the relative translational degree of freedom of the products; therefore, the substantial amount of energy released during the exothermic reaction is expected to excite the HF vibration, being consistent with the elongated H–F distance in the TS geometry. In accordance with this prediction, we observe an inverted population of the vibrational states of HF with respect to the thermal equilibrium population, peaking at $v_{HF} = 2$ in the case of the ground-state reactant, in agreement with the experiments of Nesbitt and co-workers[57] At the two lowest collision energies, a significant mode-specificity can be noticed, with the $v_{HF} = 3$ state becoming the most populated for all the vibrationally excited reactions, especially in the case of the excitation of the CH-stretching modes of ethane, where even the $v_{HF} = 4$ state emerges. This energy transfer is also reflected in the internal energy distributions of the ethyl radical at these energies (less shifted peaks). However, translational excitation, and thus shorter interaction time, prevents the excess vibrational energy to easily flow into the HF vibrational degree of freedom, resulting in

quite similar HF vibrational distributions, all peaking at $v_{HF} = 2$, at 20 kcal/mol collision energy. Nevertheless, some mode-specificity is still noticeable at this energy, reflected mainly in the enhanced $v_{HF} = 4$ probabilities in the case of the CH-stretching excitations, where even the $v_{HF} = 5$ state becomes populated.

The vibrationally resolved rotational distributions of HF, depicted in Fig. 7, are also investigated in the case of the two most populated vibrational states, $v_{HF} = 2$ and 3, and show excellent agreement with experiments for the unexcited reaction.[57] The distributions are basically independent of the ethane vibrational excitations (the fluctuations are comparable with the statistical uncertainty of these results); however, they show a minor translational energy dependence reflected in a widening shape with increasing collision energy. We can also notice that the $v_{HF} = 3$ state is rotationally colder with a maximum J_{HF} value of 15 while the $v_{HF} = 2$ rotational distribution vanishes at $J_{HF} = 20$.

CONCLUSIONS

In the present study, we investigate the vibrational mode-specific dynamics of the nine-atomic F($^2P_{3/2}$) + C_2H_6 → HF + C_2H_5 reaction and monitor the effect of five different normal-mode excitations in ethane on reactivity, mechanism, and energy utilization by performing QCT simulations on a recently developed full-dimensional MRCI-F12 analytical PES. The competition between the position of the TS along the reaction coordinate and the submerged nature of the barriers turns out to determine the shape of the excitation functions of both the F and Cl + C_2H_6 reactions. In the case of the former, the translational promotion induced by the early barrier of the reaction overcomes the reactivity-enhancing effect of interaction time, caused by the slightly negative barrier (i.e., the longer the time that the system spends near the TS-region is, the more likely the reactants convert into products). In addition, a

centrifugal barrier can also play a role by turning the slightly negative barrier for the title reaction into a slightly positive one, causing increasing reactivity with increasing collision energy. In contrast, because of the deeper negative barrier of the Cl + C_2H_6 reaction, the promoting effect of reaction time is much more apparent in this case, of course, counteracted by translational excitation. Being consistent with the Polanyi rules, the translational energy boosts more effectively the title reaction than the same amount of vibrational energy, whereas the reverse is true for the Cl + C_2H_6 reaction. We find that the angular preferences of the F + C_2H_6 reaction do not show significant mode-specificity but are clearly dependent on translational excitation: Increasing collision energy makes the HF products become more and more forward scattered, indicating an excessively dominant stripping mechanism over indirect or direct rebound pathways, prevalent at low collision energies and small impact parameters. The post-reaction energy flow evolves as follows: The excess vibrational energy pumped into ethane mostly remains in the ethyl radical, and almost all the initial translational energy is transformed into product recoil, independent of which ethane normal mode is excited, while the HF-stretching absorbs all the reaction energy released due to the elongated H–F bond at the TS. Accordingly, the HF product forms in highly excited vibrational states, which makes the ZPE-violating ethyl radicals define the effect of the ZPE-restrictions applied for the integral cross sections of the title reaction. Furthermore, we find that translational excitation hinders the considerable energy flow from the excited ethane vibrational modes to the HF vibration, observed at low collison energies, which somewhat undermines mode-specificity in the inverted HF vibrational distributions as collision energy increases.

We hope that our work will inspire further experimental and theoretical studies on the mode-specificity of this reaction family, the new benchmark systems of polyatomic reaction dynamics.

ACKNOWLEDGMENTS

AUTHOR DECLARATIONS

Conflict of Interest

The authors have no conflicts to disclose.

DATA AVAILABILITY

The data that support the findings of this study are available from the corresponding authors upon reasonable request.

REFERENCES

[1] J. C. Polanyi, Science **236**, 680 (1987).
[2] G. C. Schatz, M. C. Colton, and J. L. Grant, J. Phys. Chem. **88**, 2971 (1984).
[3] A. Sinha, M. C. Hsiao, and F. F. Crim, J. Chem. Phys. **92**, 6333 (1990).
[4] R. B. Metz, J. D. Thoemke, J. M. Pfeiffer, and F. F. Crim, J. Chem. Phys. **99**, 1744 (1993).
[5] M. J. Bronikowski, W. R. Simpson, B. Girard, and R. N. Zare, J. Chem. Phys. **95**, 8647 (1991).
[6] D. H. Zhang and J. C. Light, J. Chem. Soc., Faraday Trans. **93**, 691 (1997).
[7] W. R. Simpson, A. J. Orr-Ewing, and R. N. Zare, Chem. Phys. Lett. **212**, 163 (1993).
[8] W. R. Simpson, T. P. Rakitzis, S. A. Kandel, A. J. Orr-Ewing, and R. N. Zare, J. Chem. Phys. **103**, 7313 (1995).
[9] A. J. Orr-Ewing, W. R. Simpson, T. P. Rakitzis, S. A. Kandel, and R. N. Zare, J. Chem. Phys. **106**, 5961 (1997).
[10] S. Yoon, S. Henton, A. N. Zivkovic, and F. F. Crim, J. Chem. Phys. **116**, 10744 (2002).
[11] S. Yan, Y.-T. Wu, B. Zhang, X.-F. Yue, and K. Liu, Science **316**, 1723 (2007).
[12] W. Zhang, H. Kawamata, and K. Liu, Science **325**, 303 (2009).
[13] B. J. Braams and J. M. Bowman, Int. Rev. Phys. Chem. **28**, 577 (2009).
[14] G. Czakó, B. C. Shepler, B. J. Braams, and J. M. Bowman, J. Chem. Phys. **130**, 084301 (2009).
[15] G. Czakó and J. M. Bowman, Science **334**, 343 (2011).
[16] G. Czakó and J. M. Bowman, J. Am. Chem. Soc. **131**, 17534 (2009).
[17] J. Palma and U. Manthe, J. Chem. Phys. **146**, 214117 (2017).
[18] R. Liu, M. Yang, G. Czakó, J. M. Bowman, J. Li, and H. Guo, J. Phys. Chem. Lett. **3**, 3776 (2012).
[19] G. Czakó, J. Chem. Phys. **138**, 134301 (2013).
[20] R. Welsch and U. Manthe, J. Chem. Phys. **141**, 051102 (2014).
[21] T. Westermann, J. B. Kim, M. L. Weichman, C. Hock, T. I. Yacovitch, J. Palma, D. M. Neumark, and U. Manthe, Angew. Chem., Int. Ed. Engl. **53**, 1122 (2014).
[22] J. Qi, H. Song, M. Yang, J. Palma, U. Manthe, and H. Guo, J. Chem. Phys. **144**, 171101 (2016).
[23] F. Meng, W. Yan, and D. Wang, Phys. Chem. Chem. Phys. **14**, 13656 (2012).
[24] W. Yan, F. Meng, and D. Wang, J. Phys. Chem. A **117**, 12236 (2013).
[25] W. Yan and D. Wang, Chem. Phys. Lett. **603**, 41 (2014).
[26] N. Liu and M. Yang, J. Chem. Phys. **143**, 134305 (2015).
[27] B. Fu, X. Shan, D. H. Zhang, and D. C. Clary, Chem. Soc. Rev. **46**, 7625 (2017).
[28] B. Jiang and H. Guo, J. Chem. Phys. **138**, 234104 (2013).
[29] H. Guo and B. Jiang, Acc. Chem. Res. **47**, 3679 (2014).
[30] S. A. Kandel, T. P. Rakitzis, T. Lev-On, and R. N. Zare, J. Chem. Phys. **105**, 7550 (1996).
[31] S. A. Kandel, T. P. Rakitzis, T. Lev-On, and R. N. Zare, Chem. Phys. Lett. **265**, 121 (1997).
[32] S. Rudić, D. Ascenzi, and A. J. Orr-Ewing, Chem. Phys. Lett. **332**, 487 (2000).
[33] S. Rudić, C. Murray, D. Ascenzi, H. Anderson, J. N. Harvey, and A. J. Orr-Ewing, J. Chem. Phys. **117**, 5692 (2002).
[34] S. Rudić, C. Murray, J. N. Harvey, and A. J. Orr-Ewing, Phys. Chem. Chem. Phys. **5**, 1205 (2003).
[35] C. Murray, A. J. Orr-Ewing, R. L. Toomes, and T. N. Kitsopoulos, J. Chem. Phys. **120**, 2230 (2004).
[36] S. Rudić, C. Murray, J. N. Harvey, and A. J. Orr-Ewing, J. Chem. Phys. **120**, 186 (2004).
[37] C. Huang, W. Li, and A. G. Suits, J. Chem. Phys. **125**, 133107 (2006).
[38] S. J. Greaves, J. Kim, A. J. Orr-Ewing, and D. Troya, Chem. Phys. Lett. **441**, 171 (2007).
[39] S. J. Greaves, A. J. Orr-Ewing, and D. Troya, J. Phys. Chem. A **112**, 9387 (2008).
[40] G. Czakó, T. Győri, D. Papp, V. Tajti, and D. A. Tasi, J. Phys. Chem. A **125**, 2385 (2021).
[41] J. Li, B. Zhao, D. Xie, and H. Guo, J. Phys. Chem. Lett. **11**, 8844 (2020).
[42] B. Fu, Y.-C. Han, J. M. Bowman, L. Angelucci, N. Balucani, F. Leonori, and P. Casavecchia, Proc. Natl. Acad. Sci. U. S. A. **109**, 9733 (2012).
[43] J. Li and H. Guo, J. Chem. Phys. **143**, 221103 (2015).
[44] D. Lu, J. Behler, and J. Li, J. Phys. Chem. A **124**, 5737 (2020).
[45] D. Papp, V. Tajti, T. Győri, and G. Czakó, J. Phys. Chem. Lett. **11**, 4762 (2020).
[46] D. Papp and G. Czakó, J. Chem. Phys. **153**, 064305 (2020).
[47] D. Lu and J. Li, Theor. Chem. Acc. **139**, 157 (2020).

[48] D. Papp, J. Li, H. Guo, and G. Czakó, J. Chem. Phys. **155**, 114303 (2021).

[49] C. Rangel and J. Espinosa-Garcia, Phys. Chem. Chem. Phys. **20**, 3925 (2018).

[50] J. Espinosa-Garcia and M. Garcia-Chamorro, Phys. Chem. Chem. Phys. **20**, 26634 (2018).

[51] J. Espinosa-Garcia, M. Garcia-Chamorro, J. C. Corchado, S. Bhowmick, and Y. V. Suleimanov, Phys. Chem. Chem. Phys. **22**, 13790 (2020).

[52] J. Espinosa-Garcia, C. Rangel, J. C. Corchado, and M. Garcia-Chamorro, Phys. Chem. Chem. Phys. **22**, 22591 (2020).

[53] T. Győri and G. Czakó, J. Chem. Theory Comput. **16**, 51 (2020).

[54] Z. Xie and J. M. Bowman, J. Chem. Theory Comput. **6**, 26 (2010).

[55] W. L. Hase, *Encyclopedia of Computational Chemistry* (Wiley, New York, 1998), pp. 399–407.

[56] D. Papp, B. Gruber, and G. Czakó, Phys. Chem. Chem. Phys. **21**, 396 (2019).

[57] E. S. Whitney, A. M. Zolot, A. B. McCoy, J. S. Francisco, and D. J. Nesbitt, J. Chem. Phys. **122**, 124310 (2005).